structures (~24%).[38] We consider this to be an important achievement that points to new methodology, a paradigm of guest–host induced dipolar alignment, that can be used by chemists to engineer solid-state materials with specific properties.

Acknowledgment. The technical assistance of Barry Johnson, Louis Lardear, and Diane Peapus is acknowledged. Valuable discussions with Drs. David Thorn and Gerald Meredith are appreciated. Figures 2–4, 6, 7, 10, 12, 13, 15, and 17 were produced by using the CHEMGRAF suite of molecular modeling software, by E. Keith Davies (program MODEL, 1983, 1984) and the Chemical Crystallography Laboratory, University of Oxford (1982). These programs are used under licence.

Supplementary Material Available: Tables of positional and anisotropic thermal parameters as well as tables of bond distances and bond angles for **1–9** (63 pages). Ordering information is given on any current masthead page.

(38) Mighell, A. D.; Himes, V. L.; Rodgers, J. R. *Acta. Crystallogr., Sect. A* **1983**, *A39*, 737.

Syntheses, Structures, Selected Physical Properties, and Band Electronic Structures of the Bis(ethylenediseleno)tetrathiafulvalene Salts $(BEDSe\text{-}TTF)_2X$, $X^- = I_3^-$, AuI_2^-, and IBr_2^-

Hau H. Wang, Lawrence K. Montgomery, Urs Geiser, Leigh C. Porter, K. Douglas Carlson, John R. Ferraro, Jack M. Williams,* Carolyn S. Cariss, Rona L. Rubinstein, and Julia R. Whitworth

Chemistry and Materials Science Divisions, Argonne National Laboratory, Argonne, Illinois 60439

Michel Evain, Juan J. Novoa, and Myung-Hwan Whangbo*

Department of Chemistry, North Carolina State University, Raleigh, North Carolina 27650-8204

Received August 18, 1988

Three bis(ethylenediseleno)tetrathiafulvalene (BEDSe-TTF) based salts, $(BEDSe\text{-}TTF)_2X$ ($X^- = I_3^-$, AuI_2^-, and IBr_2^-), have been prepared by electrocrystallization and characterized by X-ray crystallography, electrical conductivity measurements, variable-temperature electron spin resonance studies, and FT-IR reflectance measurements. The triclinic (space group $P\bar{1}$) room-temperature lattice parameters for the three salts are as follows: β-$(BEDSe\text{-}TTF)_2I_3$: a = 6.781 (2) Å, b = 8.767 (3) Å, c = 16.023 (5) Å, α = 89.68 (2)°, β = 94.76 (2)°, γ = 110.66 (2)°, V = 887.9 (5) Å^3. $(BEDSe\text{-}TTF)_2AuI_2$: a = 7.614 (1) Å, b = 8.341 (2) Å, c = 15.538 (4) Å, α = 77.56 (2)°, β = 98.31 (2)°, γ = 112.71 (2)°, V = 886.9 (4) Å^3. β'-$(BEDSe\text{-}TTF)_2IBr_2$: a = 6.863 (2) Å, b = 10.065 (3) Å, c = 13.183 (3) Å, α = 87.94 (2)°, β = 100.49 (2)°, γ = 98.84 (2)°, V = 884.8 (4) Å^3. At room temperature, β-$(BEDSe\text{-}TTF)_2I_3$ is metallic and $(BEDSe\text{-}TTF)_2AuI_2$ and β'-$(BEDSe\text{-}TTF)_2IBr_2$ are semiconductors. Antiferromagnetic couplings were observed in both AuI_2^- and IBr_2^- salts at 20 and 12 K, respectively. Tight-binding band calculations were performed on the donor layers of the $(BEDSe\text{-}TTF)_2X$ salts in an attempt to understand the electrical properties. The relationships between the crystal structures, physical properties, and band electronic structures are discussed.

Introduction

The radical-cation salts of bis(ethylenedithio)tetrathiafulvalene (1, commonly abbreviated BEDT-TTF or,

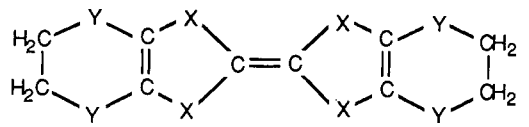

1, BEDT-TTF (ET), X = Y = S
2, BEDSe-TSeF, X = Y = Se
3, BEDSe-TTF, X = S, Y = Se

simply, ET) have been studied intensively,[1] since ambient-pressure bulk superconductivity ($T_c \sim 1.5$ K) was first discovered[2] and confirmed[3] in β-$(ET)_2I_3$ in 1984. κ-$(ET)_2Cu(NCS)_2$, the newest member of the ET family of superconductors, has an ambient-pressure superconducting transition temperature over 10 K.[4] In addition, more than half of the known ambient-pressure organic superconductors[5] are derived from ET, e.g., α_t-$(ET)_2I_3$ (T_c

(1) Williams, J. M.; Wang, H. H.; Emge, T. J.; Geiser, U.; Beno, M. A.; Leung, P. C. W.; Carlson, K. D.; Thorn, R. J.; Schultz, A. J. *Prog. Inorg. Chem.* **1987**, *35*, 51.

(2) Yagubskii, E. B.; Shchegolev, I. F.; Laukhin, V. N.; Kononovich, P. A.; Karatsovnik, M. W.; Zvarykina, A. V.; Buravov, L. I. *Pis'ma Zh. Eksp. Teor. Fiz.* **1984**, *39*, 12; *JETP Lett. (Engl. Transl.)* **1984**, *39*, 12.

(3) Williams, J. M.; Emge, T. J.; Wang, H. H.; Beno, M. A.; Copps, P. T.; Hall, L. N.; Carlson, K. D.; Crabtree, G. W. *Inorg. Chem.* **1984**, *23*, 2558.

(4) Urayama, H.; Yamochi, H.; Saito, G.; Nozawa, K.; Sugano, T.; Kinoshita, M.; Sato, S.; Oshima, K.; Kawamoto, A.; Tanaka, J. *Chem. Lett.* **1988**, 55.

(5) Other known ambient-pressure organic superconductors are derived from TMTSF,[6] DMET,[7] and MDT-TTF.[8]

0897-4756/89/2801-0140$01.50/0

~ 8 K),[9,10] ϵ_t-$(ET)_2I_3$ (T_c ~ 6–7 K),[11] β-$(ET)_2AuI_2$ (T_c = 4.98 K),[12] $(ET)_4Hg_{2.98}Br_8$ (T_c = 4.2 K),[13] θ-$(ET)_2(I_3)_{1-x}(AuI_2)_x$ (x < 0.02, T_c = 3.6 K),[14] κ-$(ET)_2(I_3)_{1-x}(AuI_2)_x$ (x < 0.006, T_c = 3.6 K),[15] γ-$(ET)_3(I_3)_{2.5}$ (T_c = 2.5 K),[16] and β-$(ET)_2IBr_2$ (T_c = 2.5 K).[17] Although there are significant crystal-structure packing differences among the various ET superconductors, a key feature for achieving superconductivity appears to be the presence of an extensive network of intermolecular S···S interactions that gives rise to two-dimensional (2D) metallic character. Tight-binding band calculations on the donor layers of several of the salts support this viewpoint.[1,18] In the search for new electron-donor molecules to produce organic superconductors with even higher T_c's, an appealing approach is to replace some or all of the sulfur atoms of ET with chalcogens of higher atomic number such as selenium, since the increased overlap expected from the larger selenium atoms could facilitate intermolecular interactions and promote increased dimensionality in the transport properties of derived charge-transfer salts. Moreover, the greater size of the selenium atoms should lead to an increase in the unit-cell volume in systems that remain isostructural upon selenium substitution, and a reduction in the on-site Coulomb energy could result. The completely substituted selenium analogue of ET, BEDSe-TSeF (**2**), has been prepared previously.[19] However, the limited solubility of **2** has hampered the systematic investigation of this interesting donor. Furthermore, its redox behavior is somewhat different from ET: $E_{1/2}{}^1$ is roughly 0.1 V higher than that of the ET value, and the difference in first and second oxidation potentials in **2** is approximately 0.1 V smaller. The reduced difference between $E^1{}_{1/2}$ and $E^2{}_{1/2}$ tends to favor formation of 1:1 salts, and the majority of BEDSe-TSeF salts that have been reported (X$^-$ = $AuBr_2^-$, PF_6^-, ClO_4^-, ReO_4^-)[19,20] have that stoichiometry. To date, only one 2:1 salt of **2** has appeared in the literature, $(BEDSe\text{-}TSeF)_2AuBr_2$, and it is a semiconductor.[21]

In the present study we describe the syntheses, crystal structures, selected physical properties, and band electronic structures of three new 2:1 radical-cation salts of a mixed sulfur–selenium analogue of ET in which the four outer sulfur atoms are replaced by selenium, $(BEDSe\text{-}TTF)_2X$ (**3**). Although we have prepared BEDSe-TTF salts with several different types of counterions, all of the salts discussed here contain linear anions (X$^-$ = I_3^-, AuI_2^-, and IBr_2^-). These three radical-cation salts are of particular interest, because their β-phase ET counterparts are all ambient-pressure superconductors. This is noteworthy, since selenium analogues of sulfur heterocycles are frequently isostructural crystallographically.[22]

The BEDSe-TTF (**3**) donor molecule has a number of advantages over that of BEDSe-TSeF (**2**). The replacement of only four of the sulfur atoms of ET by selenium atoms yields a donor with acceptable solubility properties. For example, the solubility of **3** in tetrahydrofuran (THF) is roughly half that of ET. An even more desirable feature of **3** is that the central TTF portion of the ET molecule is left intact. This is advantageous, because tight-binding band calculations suggest[1,18] that the interstack S···S interactions between the TTF sulfur atoms are a major factor in establishing the two-dimensional metallic network in the superconducting β-$(ET)_2X$ salts. It is also worth noting that the first and second oxidation potentials of **3** are very similar to those of ET. Syntheses of **3** have been published by Lee[23] and Nigrey.[24,25] A slightly different synthetic route was employed here. The molecular structure of the 1:1 triiodide salt of **3**, $BEDSe\text{-}TTF^+I_3^-$, has been reported recently.[25] Brief references have also been made to semiconducting IBr_2^- and AuI_2^- salts of **3**, but the molecular stoichiometry was not specified.[23]

Experimental Section

Synthesis. The synthetic procedures were adopted from the literature with several modifications.[23,24] No attempt was made to optimize the yields, because a new and improved method of preparation[26] was being developed at the time that this work was carried out. All chemicals (reagent grade) were purchased from Aldrich except for the vinylene trithiocarbonate, which was purchased from Fluka.

4,5-Ethylenediseleno-1,3-dithiole-2-thione (4). The reaction was carried out under Ar employing standard Schlenk techniques. Lithium diisopropylamine was generated by dropping *n*-butyllithium in hexane (19 mL, 2.5 M, 47.5 mmol) into 40 mL of THF solution containing 5.3 mL of diisopropylamine (37.5 mmol) that was cooled in a dry ice/acetone bath (−70 °C). The reaction mixture was stirred at −70 °C for 45 min before 2.46 g of vinylene trithiocarbonate (18.3 mmol) in 10 mL of THF was added dropwise. The resulting light brown solution was stirred at −70 °C for 2 h. About 2.9 g of selenium powder was suspended in THF with ultrasonic agitation and was added to the above mixture in one portion. The resulting deep red solution was warmed to room temperature overnight and evaporated to dryness under reduced pressure. The residue was redissolved in methanol. Approximately 6.3 mL of ethylene dibromide (73 mmol) was added dropwise. After stirring at room temperature for 2 h, the mixture was filtered. The filtrate was concentrated and was chromato-

(6) TMTSF is tetramethyltetraselenafulvalene. Bechgaard, K.; Carneiro, K.; Rasmussen, F. B.; Olsen, M.; Rindorf, G.; Jacobsen, C. S.; Pedersen, H. J.; Scott, J. C. *J. Am. Chem. Soc.* **1981**, *103*, 2440.

(7) DMET is dimethyl(ethylenedithio)diselenadithiafulvalene. Ikemoto, I. In *Superconducting Materials*; Nakajima, S., Fukuyama, H., Eds.; JJAP Series 1, 1988; p 170.

(8) MDT-TTF is (methylenedithio)tetrathiafulvalene. Papavassiliou, G. C.; Mousdis, G. A.; Zambounis, J. S.; Terzis, A.; Hountas, A.; Hilti, B.; Mayer, C. W.; Pfeiffer, J. *Synth. Met.*, in press.

(9) Baram, G. O.; Buravov, L. I.; Degtyarev, L. S.; Kozlov, M. E.; Laukhin, V. N.; Laukhina, E. E.; Onishchenko, V. G.; Pokhodnya, K. I.; Shienkman, M. K.; Shibaeva, R. P.; Yagubskii, E. B. *JETP Lett.* (*Engl. Transl.*) **1986**, *44*, 376.

(10) Schweitzer, D.; Bele, P.; Brunner, H.; Gogu, E.; Haeberlen, U.; Hennig, I.; Klutz, I.; Swietlik, R.; Keller, H. J. *Z. Phys.* **1987**, *B67*, 489.

(11) Merzhanov, V. A.; Kostyuchenko, E. E.; Laukhin, V. N.; Lobkovskaya, R. M.; Makova, M. K.; Shibaeva, R. P.; Shchegolev, I. F.; Yagubskii, E. B. *JETP Lett.* (*Engl. Transl.*) **1985**, *41*, 179.

(12) Wang, H. H.; Beno, M. A.; Geiser, U.; Firestone, M. A.; Webb, K. S.; Nuñez, L.; Crabtree, G. W.; Carlson, K. D.; Williams, J. M.; Azevedo, L. J.; Kwak, J. F.; Schirber, J. E. *Inorg. Chem.* **1985**, *24*, 2465.

(13) Lyubovskaya, R. N.; Zhilyaeva, E. I.; Pesotskii, S. I.; Lyubovskii, R. B.; Atovmyan, L. O.; D'yachenko, O. A.; Takhirov, T. G. *JETP Lett.* (*Engl. Trans.*) **1987**, *46*, 188.

(14) Kobayashi, H.; Kato, R.; Kobayashi, A.; Nishio, Y.; Kajita, K.; Sasaki, W. *Chem. Lett.* **1986**, *789*, 833.

(15) Kobayashi, A.; Kato, R.; Kobayashi, H.; Moriyama, S.; Nishio, Y.; Kajita, K.; Sasaki, W. *Chem. Lett.* **1987**, 459.

(16) Shibaeva, R. P.; Kaminskii, V. F.; Yagubskii, E. B. *Mol. Cryst. Liq. Cryst.* **1985**, *119*, 361.

(17) Williams, J. M.; Wang, H. H.; Beno, M. A.; Emge, T. J.; Sowa, L. M.; Copps, P. T.; Behroozi, F.; Hall, L. N.; Carlson, K. D.; Crabtree, G. W. *Inorg. Chem.* **1984**, *23*, 3839.

(18) (a) Whangbo, M.-H.; Williams, J. M.; Leung, P. C. W.; Beno, M. A.; Emge, T. J.; Wang, H. H.; Carlson, K. D.; Crabtree, G. W. *J. Am. Chem. Soc.* **1985**, *107*, 5815. (b) Whangbo, M.-H.; Williams, J. M.; Leung, P. C. W.; Beno, M. A.; Emge, T. J.; Wang, H. H. *Inorg. Chem.* **1985**, *24*, 3500.

(19) Lee, V. Y.; Engler, E. M.; Schumaker, R. R.; Parkin, S. S. P. *J. Chem. Soc., Chem. Commun.* **1983**, *5*, 235.

(20) Kato, R.; Kobayashi, H.; Kobayashi, A.; Sasaki, Y. *Chem. Lett.* **1985**, 1231.

(21) Kato, R.; Kobayashi, H.; Kobayashi, A. *Chem. Lett.* **1986**, 785.

(22) Hargittai, I.; Rozsondai, B. In *The Chemistry of Organic Selenium and Tellurium Compounds*; Patai, S., Rappoport, Z., Eds.; John Wiley: New York, 1986; Vol. 1, p 63.

(23) Lee, V. Y. *Synth. Met.* **1987**, *20*, 161.

(24) Nigrey, P. J.; Morosin, B.; Kwak, J. F. In *Novel Superconductivity*; Wolf, S. A., Kresin, V. Z., Eds.; Plenum, New York, 1987; p 171.

(25) Nigrey, P. J.; Morosin, B.; Duesler, E. *Synth. Met.*, in press.

(26) Kini, A. M.; Gates, B. D.; Beno, M. A.; Williams, J. M. *J. Chem. Soc., Chem. Commun.*, submitted for publication.

Table I. Electrocrystallization Syntheses of $(BEDSe\text{-}TTF)_2X$ Salts

	donor, mM	anion, mM	current density, $\mu A/cm^2$	ESR line width,[b] G
β-$(BEDSe\text{-}TTF)_2I_3$[a] (6)	0.49	36.1	0.8	47–56
$(BEDSe\text{-}TTF)_2AuI_2$[a] (7)	0.47	19.8	0.7	16–19
β'-$(BEDSe\text{-}TTF)_2IBr_2$ (8)	0.54	38.6	0.7	23–29

[a] Major phase obtained from electrocrystallization. [b] Room temperature.

graphed on an alumina column with CH_2Cl_2/hexane (1:1). The crude product was recrystallized from $CHCl_3$ once to give 0.29 g of dark yellow crystals of **4** (5% yield), mp 159 °C. Anal. Calcd for $C_5H_4S_3Se_2$: C, 18.87; H, 1.27; S, 30.23. Found: C, 18.94; H, 1.40; S, 30.43. MS parent m/e 320; IR (KBr, cm^{-1}) 1454 (m), 1400 (m), 1260 (s), 1052 (vs), 1034 (vs), 889 (w), 809 (s), 520 (m), 448 (m), 416 (m).

4,5-Ethylenediseleno-1,3-dithiol-2-one (5). A 15-mL $CHCl_3$ solution containing 0.29 g of **4** was added to a 12-mL glacial acetic acid solution containing 0.34 g of $Hg(OAc)_2$. The mixture was refluxed for 3.5 h. Na_2SO_4 was added to the cooled mixture, and the resulting slurry was filtered. Na_2CO_3 and a small amount of distilled water were added to the filtrate until no bubbles were observed. The organic layer was separated and filtered through a short pad of alumina powder and concentrated by using a rotatory evaporator. The crude product was recrystallized from absolute EtOH to give 0.17 g of off-white crystals of **5** (60% yield), mp 105–106 °C. MS parent m/e 304; IR (KBr, cm^{-1}) 1735 (m), 1639 (vs), 1563 (m), 1480 (m), 1410 (m), 1258 (w), 866 (m), 783 (m), 699 (m), 439 (w).

Bis(ethylenediseleno)tetrathiafulvalene, BEDSe-TTF (3). A solution of 0.15 g of **5** in 10 mL of trimethyl phosphite was refluxed for 2 h. The resulting orange solution was cooled in an ice/acetone bath for 20 min. The crude product was filtered and recrystallized from $CHCl_3$ to give 30 mg of BEDSe-TTF (20% yield), mp ~230 °C (dec).

Electrocrystallization Synthesis of $(BEDSe\text{-}TTF)_2X$, $X^- = I_3^-$ (6), AuI_2^- (7), IBr_2^- (8). All three salts were prepared from the donor molecule BEDSe-TTF in the presence of NBu_4X supporting electrolytes at 23.0 ± 0.2 °C in tetrahydrofuran solvent following standard electrocrystallization procedures.[27] The concentration of each reactant, current density employed, and the room-temperature electron spin resonance (ESR) line width of each salt are listed in Table I. For the I_3^- anion, a minor phase has been observed, viz., a 1:1 salt, $(BEDSe\text{-}TTF)I_3$, which has been reported previously.[25]

X-ray Diffraction. Single-crystal diffraction data were collected on a Nicolet P3/F (compounds **6** and **7**) or a Syntex $P2_1$ diffractometer (compound **8**). The lattice constants were determined from the angular settings of 25–30 well-centered Bragg reflections in the range $20° < 2\theta < 30°$. Crystallographic data are given in Table II; further details of the data collection are deposited in the supplementary material (see paragraph at the end of the paper). The crystal structures were solved by direct methods and completed by use of Fourier methods.[28] In the full-matrix least-squares refinement,[29] positional parameters and anisotropic temperature factors were refined for all non-hydrogen atoms except where noted in the tables. Hydrogen atoms were included at fixed, calculated positions ($d_{H\text{-}C}$ = 1.0 Å) for the AuI_2^- compound. In the case of **6**, a small secondary extinction correction parameter was refined. Compounds **7** and **8** have relatively high agreement factors, indicating structural problems. In the case of **7**, almost all the discrepancy between observed and calculated structure factors can be traced to features on the final difference map (both positive and negative, up to 7 e $Å^{-3}$) in the vicinity of the anion atoms,[30] indicating disorder. However, no chemically plausible scheme could be conceived to model the disorder. Similarly, in **8** the largest excursions on the difference map are found near the anion.

Table II. Crystallographic Data for $(BEDSe\text{-}TTF)_2X$ Salts

	$X = I_3^-$ (6)	$X = AuI_2^-$ (7)	$X = IBr_2^-$ (8)
chem formula	$C_{20}H_{16}S_8Se_8I_3$	$C_{20}H_{16}S_8Se_8AuI_2$	$C_{20}H_{16}S_8Se_8IBr_2$
a, Å	6.781 (2)	7.614 (1)	6.863 (2)
b, Å	8.767 (3)	8.341 (2)	10.065 (3)
c, Å	16.023 (5)	15.538 (4)	13.183 (3)
α, deg	89.68 (2)	77.56 (2)	87.94 (2)
β, deg	94.76 (2)	98.31 (2)	100.49 (2)
γ, deg	110.66 (2)	112.71 (2)	98.84 (2)
V, $Å^3$	887.9 (5)	886.9 (4)	884.8 (4)
Z	1	1	1
formula wt	1525.2	1595.3	1431.2
space group	$P\bar{1}$	$P\bar{1}$	$P\bar{1}$
T, °C	25 (2)	25 (2)	25 (2)
γ, Å	0.71073	0.71073	0.71073
d(calcd), g cm^{-3}	2.852	2.987	2.686
μ, cm^{-1}	112.0	144.6	117.5
transm coeff	0.107–0.242	0.091–0.324	a
R (F_o)	0.047	0.085	0.085
R_w (F_o)	0.040	0.088	0.110

[a] Empirical ψ-scan absorption correction.

Physical Property Measurements. The temperature dependence of the electrical resistivity of the $(BEDSe\text{-}TTF)_2X$ salts was measured by the use of a standard four-probe technique for **6** and **7** and a two-probe technique for **8** because of the smaller size of these crystals. The ESR experiments employed an IBM ER-200 spectrometer with a TE_{102} rectangular cavity and an Oxford Instrument EPR-900 flow cryostat with an ITC4 temperature controller. Room-temperature FT-IR reflectance measurements were made with a Digilab FTS-40 purged spectrometer interfaced with a UMA 300-A microscope at a resolution of 4 cm^{-1}. The cadmium–mercury–telluride detector was used, and a typical spectrum was acquired with 256 scans. A Kramers–Kronig transformation was applied to all reflectance spectra to convert them into absorption spectra.

Results and Discussion

Molecular Structures and Conformations. The final atomic coordinates and equivalent isotropic thermal parameters for the three $(BEDSe\text{-}TTF)_2X$ salts, where $X^- = I_3^-$ (**6**), AuI_2^- (**7**), and IBr_2^- (**8**), are given in Table III. Bond distances and bond angles are provided in Table IV. The labeling scheme as well as the molecular conformations of compounds **6**, **7**, and **8** are shown in Figure 1. The tetrathiafulvalene portions of **6**, **7**, and **8** have structural parameters that are within experimental error of the corresponding parameters in ET salts possessing donor molecules with $+^1/_2$ formal charges.[1] $(BEDSe\text{-}TTF)_2AuI_2$ has two crystallographically independent BEDSe-TTF units, but no differences could be discerned between related bond lengths in the two molecules within the precision of the structure determination. The most significant changes in bond lengths in going from ET to BEDSe-TTF occur directly at the sites where selenium substitution takes place: the C–Se bonds are about 0.2 Å longer than typical C–S bonds. This modest increase in length may have a profound influence on molecular conformation and, indirectly, on crystal packing. Three types of conformations are commonly observed in the six-membered rings of ET salts. They are shown schematically in Figure 2. Conformation a is found exclusively in the superconducting β-phase $(ET)_2X$ salts.[1] As shown in Figure 1, however, the ethylene portions of **6**, **7**, and **8** do not adopt conformation a. Although some of the ethylene groups of **6** and **8** are disordered, a clear preference for conformations b and c is observed in **6**, **7**, and **8**. Ab initio SCF-MO/MP2 calculations were carried out on conformations a, b, and c

(27) Williams, J. M. *Inorg. Synth.* **1986**, *24*, 136.
(28) The computer programs were local modifications of: Strouse, C. *UCLA Crystallographic Package*, University of California, Los Angeles, 1978 and 1986.
(29) Atomic scattering factors from: *International Tables for X-ray Crystallography*; Kynoch Press: Birmingham, UK: 1974; Vol IV.
(30) A contoured difference map has been deposited as supplementary material.

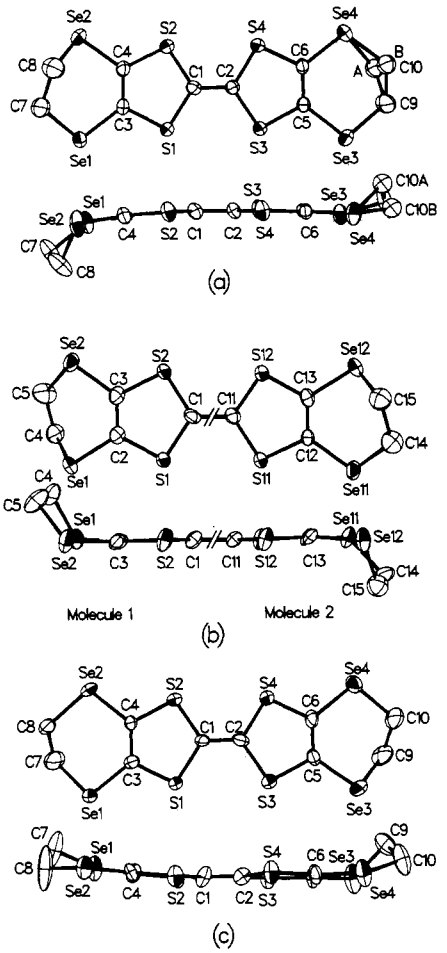

Figure 1. BEDSe-TTF molecules (top and side views) in (BEDSe-TTF)$_2$X salts: (a) X$^-$ = I_3^-; (b) X$^-$ = AuI_2^-; (c) X$^-$ = IBr_2^-. Ellipsoids are drawn at the 50% probability level and hydrogen atoms are omitted for clarity. In (b), the unique halves of each molecule were combined on the same figure by a translation $^1/_2a + {}^1/_2b$.

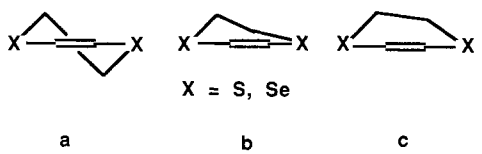

Figure 2. Schematic representation of three conformations adopted by the six-membered rings of ET and BEDSe-TTF salts.

(Figure 2) for X = S and Se employing the 3-21G basis set.[31] The most stable conformation of the three for X = S was a, and the most stable for X = Se was c. Whether internal factors, i.e., the conformational consequences of substituting selenium for sulfur, are solely responsible for the presence of only b- and c-type conformations in the BEDSe-TTF salts is not clear. The variety of conformations that are observed in the radical cation salts of ET[1] indicates that intermolecular crystal packing interactions make an important contribution to donor conformations in the solid state.

Crystal Packing. All three compounds crystallize in the triclinic space group $P\bar{1}$, with comparable unit cell volumes and axial lengths (Table II). It is not surprising, therefore, that the structures of **6**, **7**, and **8** possess some similarities. However, they are by no means isostructural,

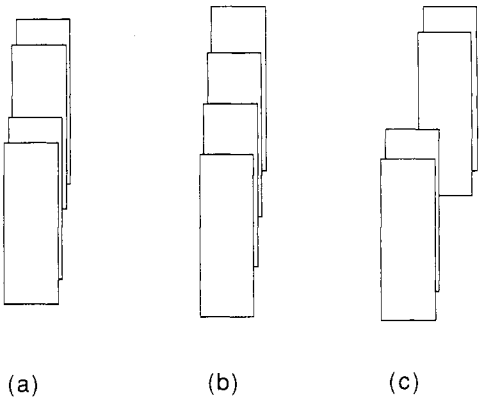

Figure 3. Schematic representation of the different donor molecule stacking motifs in (BEDSe-TTF)$_2$X salts: (a) X$^-$ = I_3^- (β); (b) X$^-$ = AuI_2^-; (c) X$^-$ = IBr_2^- (β'). The corners of each rectangle are formed by the selenium atoms of a single donor molecule.

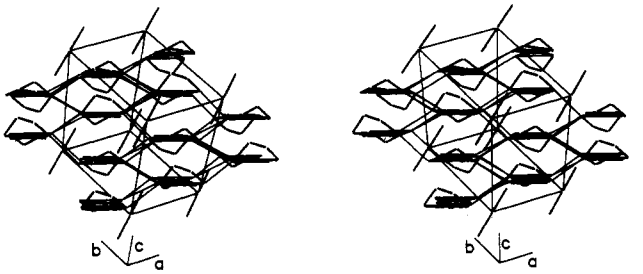

Figure 4. Stereoview of the crystal packing of β-(BEDSe-TTF)$_2$I$_3$ (**6**), as projected approximately along the long donor molecule direction. Short intermolecular contacts (Se···Se < 3.8 Å, Se···S < 3.7 Å, S···S < 3.6 Å) are indicated by thinner lines.

as can be seen from the schematic comparison in Figure 3. The distinct features of each system are described below. The structures all contain layers of BEDSe-TTF donor molecules parallel to the *ab* plane, alternating along *c* with anion layers. The longest of the three molecular axes, while not exactly perpendicular to the donor plane of the BEDSe-TTF molecule, forms the largest angle to the *ab* plane. Within the donor plane, it is possible to discern a stacking direction, approximately along the normal of the donor molecular plane, which in all three structures follows the *a* + *b* diagonal direction. Intermolecular Se···Se, Se···S, and S···S contacts shorter than the sum of the van der Waals radii (1.8 Å for S, 1.9 Å for Se)[32] occur between the stacks, as indicated in Table V. These contacts are known to be important in determining the electrical properties of organic metals. In the case of β-(BEDSe-TTF)$_2$I$_3$, the crucial S···S contacts between the TTF centers in neighboring donor molecules are significantly longer than those in β-(ET)$_2$I$_3$. In the AuI_2^- and IBr_2^- salts of BEDSe-TTF there are very few short chalcogen nonbonded distances.

β-(BEDSe-TTF)$_2$I$_3$ (6). Radical-cation salt **6** is the second crystallographic phase found in the BEDSe-TTF/I_3^- system. Nigrey[25] has recently reported the preparation of the 1:1 salt, (BEDSe-TTF)I$_3$, employing similar synthesis conditions. Triiodide **6** is the only 2:1 salt of the three reported in the present work to remain isostructural (Figure 4) with the β-(ET)$_2$X family of compounds (X$^-$ = I_3^-, AuI_2^-, IBr_2^-).[3,12,17] The unit cell volume of **6** is larger than that of the β-(ET)$_2$I$_3$ but smaller than (PT)$_2$I$_3$ [PT is bis(propylenedithio)tetrathiafulvalene].[33]

(31) Hehae, W. J.; Radom, L.; Schleyev, P. V. R.; Pople, J. A. *Ab. Initio Molecular Orbital Theory*; John Wiley; New York, 1986; p 86.

(32) Bondi, A. J. *Chem. Phys.* **1964**, *68*, 441.

(33) Kobayashi, H.; Takahashi, M.; Kato, R.; Kobayashi, A.; Sasaki, Y. *Chem. Lett.* **1984**, 1331.

Table III. Atomic Coordinates and Equivalent Isotropic Thermal Parameters[a] of (BEDSe-TTF)$_2$X Salts

atom	x	y	z	10^4U_{eq}
		β-(BEDSe-TTF)$_2$I$_3$ (6)		
I1	0.0000	0.0000	0.0000	520 (2)
I2	0.42680 (8)	0.23791 (6)	−0.00244 (3)	649 (2)
Se1	0.14148 (11)	0.36673 (8)	0.80395 (4)	522 (3)
Se2	−0.26927 (11)	0.53330 (10)	0.77795 (5)	570 (3)
Se3	0.71836 (10)	0.89958 (8)	0.32792 (4)	455 (2)
Se4	0.29527 (11)	1.06659 (8)	0.30073 (4)	490 (2)
S1	0.2649 (2)	0.5259 (2)	0.63498 (9)	397 (5)
S2	−0.0698 (2)	0.6640 (2)	0.61243 (9)	385 (5)
S3	0.4673 (2)	0.7154 (2)	0.46881 (9)	393 (5)
S4	0.1319 (2)	0.8533 (2)	0.45155 (9)	395 (5)
C1	0.1561 (8)	0.6490 (7)	0.5767 (3)	332 (19)
C2	0.2427 (8)	0.7304 (7)	0.5080 (3)	311 (18)
C3	0.0872 (9)	0.4873 (7)	0.7122 (3)	306 (18)
C4	−0.0674 (9)	0.5477 (7)	0.7101 (3)	335 (19)
C5	0.4786 (8)	0.8539 (6)	0.3884 (3)	299 (18)
C6	0.3231 (8)	0.9151 (6)	0.3810 (3)	298 (18)
C7	0.0232 (13)	0.4469 (10)	0.8947 (4)	711 (33)
C8	−0.0619 (14)	0.5780 (10)	0.8753 (4)	756 (35)
C9	0.6383 (14)	1.0004 (12)	0.2293 (5)	938 (42)
C10A	0.4205 (14)	0.9803 (12)	0.2115 (6)	456 (22)[b]
C10B	0.500 (5)	1.086 (4)	0.228 (2)	456[c]
		(BEDSe-TTF)$_2$AuI$_2$ (7)		
Au	0.5000	0.0000	0.0000	358 (4)
I	0.7745 (2)	0.2911 (2)	0.00577 (10)	548 (7)
Se1	−0.0071 (3)	0.3538 (3)	0.71009 (14)	423 (8)
Se2	0.2679 (3)	0.0991 (3)	0.78623 (14)	487 (8)
S1	0.2522 (7)	0.5130 (7)	0.5508 (3)	439 (20)
S2	0.4914 (7)	0.2996 (7)	0.6183 (3)	428 (19)
C1	0.445 (3)	0.462 (3)	0.5342 (12)	382 (74)
C2	0.192 (3)	0.360 (2)	0.6479 (12)	333 (68)
C3	0.299 (3)	0.264 (2)	0.6803 (12)	363 (71)
C4	0.154 (3)	0.380 (3)	0.8222 (14)	550 (92)
C5	0.215 (4)	0.235 (3)	0.862 (2)	725 (115)
Se11	0.2297 (3)	0.4047 (3)	0.21421 (14)	486 (8)
Se12	0.5035 (3)	0.1489 (3)	0.28771 (15)	489 (9)
S11	0.0080 (7)	0.1190 (7)	0.3822 (3)	417 (19)
S12	0.2447 (7)	−0.0110 (7)	0.4476 (3)	437 (20)
C11	0.053 (3)	0.037 (2)	0.4650 (12)	343 (70)
C12	0.199 (3)	0.240 (3)	0.3196 (11)	352 (70)
C13	0.306 (3)	0.142 (3)	0.3519 (12)	350 (70)
C14	0.282 (3)	0.273 (3)	0.1363 (15)	557 (93)
C15	0.333 (3)	0.119 (3)	0.180 (2)	524 (59)[b]
		β′-(BEDSe-TTF)$_2$IBr$_2$ (8)		
I	0.0000	0.0000	0.0000	414 (6)
Br	0.0929 (3)	0.2374 (2)	−0.09554 (15)	525 (7)
Se1	0.0022 (2)	−0.6483 (2)	0.15660 (14)	477 (7)
Se2	−0.4782 (2)	−0.5382 (2)	0.19169 (13)	412 (6)
Se3	0.6712 (3)	−0.0979 (2)	0.7110 (2)	628 (8)
Se4	0.2002 (3)	0.0163 (2)	0.7285 (2)	546 (7)
S1	0.1681 (6)	−0.4763 (4)	0.3501 (3)	356 (13)
S2	−0.2082 (6)	−0.3873 (4)	0.3731 (3)	363 (13)
S3	0.4066 (6)	−0.2787 (4)	0.5369 (3)	390 (14)
S4	0.0317 (6)	−0.1797 (4)	0.5505 (3)	405 (14)
C1	0.047 (2)	−0.373 (2)	0.4149 (11)	355 (52)
C2	0.148 (2)	−0.290 (2)	0.4905 (12)	342 (50)
C3	−0.041 (2)	−0.537 (2)	0.2614 (12)	350 (52)
C4	−0.218 (2)	−0.4951 (14)	0.2715 (12)	293 (48)
C5	0.416 (2)	−0.157 (2)	0.6298 (12)	397 (56)
C6	0.244 (2)	−0.113 (2)	0.6351 (12)	373 (54)
C7	−0.244 (3)	−0.643 (3)	0.059 (2)	920 (115)
C8	−0.423 (3)	−0.667 (3)	0.096 (2)	1074 (125)
C9	0.627 (3)	0.088 (2)	0.716 (2)	571 (74)
C10	0.475 (3)	0.105 (2)	0.777 (2)	707 (87)

[a] The complete temperature factor is $\exp(-8\pi^2U_{eq}\sin^2\theta/\lambda^2)$, where $U_{eq} = {}^1/_3\sum_{ij}U_{ij}a_i^*a_j^*\mathbf{a}_i\cdot\mathbf{a}_j$ in units of Å^2. [b] U_{iso}. [c] C10A and C10B are half occupied; U_{iso} is constrained to be equal.

If projected along the direction normal to the molecular plane (see Figure 3), consecutive molecules exhibit some weak dimerization in their relative displacements along the long molecular axis (1.0 and 4.5 Å within and between dimers, respectively), whereas the displacements along the short axis are negligible (less than 0.2 Å). A slight dimerization is also noted in the intrastack direction: the molecular planes of the donor molecules alternate at separations of 3.57 and 3.75 Å.

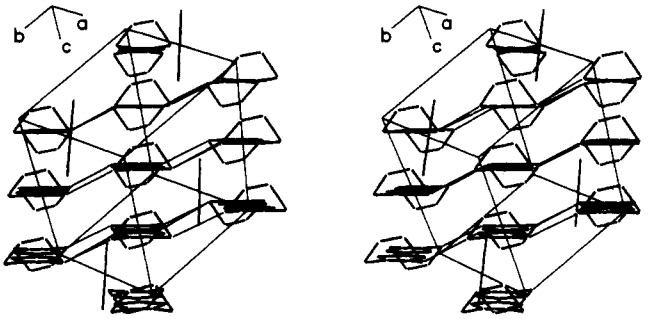

Figure 5. As in Figure 4, for (BEDSe-TTF)$_2$AuI$_2$ (7).

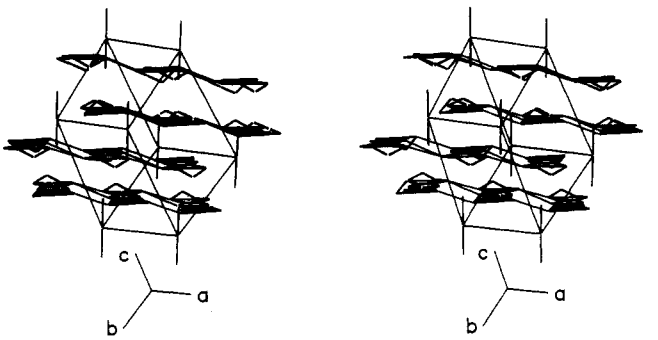

Figure 6. As in Figure 4, for β′-(BEDSe-TTF)$_2$IBr$_2$ (8).

(BEDSe-TTF)$_2$AuI$_2$ (7). In contrast to the other two structures (6 and 8) reported here, in which the donor molecules are located on general positions, the two crystallographically independent BEDSe-TTF molecules in the AuI_2^- salt (Figure 5) are located on centers of inversion (molecule 1 at ${}^1/_2,{}^1/_2,{}^1/_2$, molecule 2 at $0,0,{}^1/_2$). Furthermore, the two molecules are oriented essentially parallel to each other, such that a translation ${}^1/_2a + {}^1/_2b$ virtually superimposes the two molecules (within no more than 0.1 Å, even on the ethylene end groups).[34] Due to symmetry, the donor molecules in each stack are not dimerized but are uniformly spaced with a larger intrastack separation of 3.7 Å.

β′-(BEDSe-TTF)$_2$IBr$_2$ (8). The IBr_2^- salt (Figures 3 and 6) is isostructural with the β′-(ET)$_2$X family of compounds ($X^- = ICl_2^-$, $BrICl^-$, $AuCl_2^-$).[35,36] The donor molecules in 8 are significantly more dimerized than those in 6 (see Figure 3). This dimerization results in strong interactions within a dimer (3.5 Å apart) and weak interactions between dimers (separation 4.7 Å). Another general feature of the β′-type structure is that the pronounced donor molecule dimerization allows more intimate donor–anion contacts than in the other two structure types. The crossover from the β- to the β′-structural type with decreasing linear anion size that takes place between IBr_2^- and $BrICl_2^-$ in the ET system is shifted toward larger anions, i.e., larger than IBr_2^- when the larger donor

(34) Every effort was made to find hidden symmetry elements that would render the molecules equivalent. However, the location of the AuI_2^- counterions breaks the pseudosymmetry.

(35) Emge, T. J.; Wang, H. H.; Leung, P. C. W.; Rust, P. R.; Cook, J. D.; Jackson, P. L.; Carlson, K. D.; Williams, J. M.; Whangbo, M.-H.; Venturini, E. L.; Schirber, J. E.; Azevedo, L. J.; Ferraro, J. R. *J. Am. Chem. Soc.* **1986**, *108*, 695.

(36) Emge, T. J.; Wang, H. H.; Bowman, M. K.; Pipan, C. M.; Carlson, K. D.; Beno, M. A.; Hall, L. N.; Anderson, B. A.; Williams, J. M.; Whangbo, M.-H. *J. Am. Chem. Soc.* **1987**, *109*, 2016.

Table IV. Bond Lengths and Angles for (BEDSe-TTF)$_2$X Salts

interatomic dist, Å		bond angles, deg		interatomic dist, Å		bond angles, deg	
			β-(BEDSe-TTF)$_2$I$_3$ (6)				
I1–I2	2.9131 (11)	C3–Se1–C7	101.8 (3)	S4–C6	1.730 (5)	S1–C3–Se1	115.6 (3)
Se1–C3	1.892 (5)	C4–Se2–C8	93.7 (3)	C1–C2	1.368 (7)	C3–C4–S2	117.3 (4)
Se1–C7	1.963 (7)	C5–Se3–C9	101.6 (3)	C3–C4	1.331 (8)	C3–C4–Se2	125.1 (4)
Se2–C4	1.889 (5)	C6–Se4–C10A	94.4 (3)	C5–C6	1.339 (7)	S2–C4–Se2	117.4 (3)
Se2–C8	1.954 (8)	C6–Se4–C10B	105 (1)	C7–C8	1.478 (10)	C6–C5–S3	116.4 (4)
Se3–C5	1.881 (5)	C1–S1–C3	95.1 (3)	C9–C10B	1.39 (3)	C6–C5–Se3	129.9 (4)
Se3–C9	1.938 (7)	C1–S2–C4	95.3 (3)	C9–C10A	1.428 (12)	S3–C5–Se3	113.6 (3)
Se4–C6	1.890 (5)	C2–S3–C5	95.3 (2)			C5–C6–S4	117.7 (4)
Se4–C10B	1.85 (3)	C2–S4–C6	95.7 (3)			C5–C6–Se4	125.7 (4)
Se4–C10A	2.001 (9)	C2–C1–S1	123.1 (4)			S4–C6–Se4	116.6 (3)
S1–C1	1.737 (5)	C2–C1–S2	121.8 (4)			C8–C7–Se1	117.6 (5)
S1–C3	1.748 (5)	S1–C1–S2	115.2 (3)			C7–C8–Se2	114.9 (5)
S2–C1	1.727 (5)	C1–C2–S3	123.1 (4)			C10B–C9–Se3	124 (1)
S2–C4	1.745 (5)	C1–C2–S4	122.1 (4)			C10A–C9–Se3	118.4 (6)
S3–C2	1.741 (5)	S3–C2–S4	114.8 (3)			C9–C10A–Se4	115.0 (7)
S3–C5	1.753 (5)	C4–C3–S1	117.0 (4)			C9–C10B–Se4	127 (2)
S4–C2	1.729 (5)	C4–C3–Se1	127.5 (4)				
			(BEDSe-TTF)$_2$AuI$_2$ (7)				
Au–I	2.529 (2)	C2–Se1–C4	93.1 (8)	Se12–C15	1.96 (2)	C12–Se11–C14	99.7 (8)
Se1–C2	1.89 (2)	C3–Se2–C5	98.8 (9)	S11–C11	1.75 (2)	C13–Se12–C15	91.2 (8)
Se1–C4	1.98 (2)	C1–S1–C2	95.1 (8)	S11–C12	1.75 (2)	C11–S11–C12	96.4 (8)
Se2–C3	1.88 (2)	C1–S2–C3	95.3 (8)	C12–C11	1.73 (2)	C11–S12–C13	96.0 (8)
Se2–C5	1.98 (2)	C1′–C1–S1	124 (2)	S12–C13	1.73 (2)	C11′–C11–S11	122 (2)
S1–C1	1.75 (2)	C1′–C1–S2	121 (2)	C11–C11′	1.34 (3)	C11′–C11–S12	125 (2)
S1–C2	1.74 (2)	S1–C1–S2	114 (1)	C12–C13	1.34 (2)	S12–C11–S11	114 (1)
S2–C1	1.77 (2)	C3–C2–S1	119 (1)	C14–C15	1.49 (3)	C13–C12–S11	115 (1)
S2–C3	1.76 (2)	C3–C2–Se1	122 (1)			C13–C12–Se11	126 (1)
C1–C1′[a]	1.34 (4)	S1–C2–Se1	118.6 (9)			S11–C12–Se11	118.5 (9)
C2–C3	1.33 (2)	C2–C3–S2	116 (1)			C12–C13–S12	119 (1)
C4–C5	1.45 (3)	C2–C3–Se2	127 (1)			C12–C13–Se12	121 (1)
Se11–C12	1.88 (2)	S2–C3–Se2	117.4 (9)			S12–C13–Se12	119 (1)
Se11–C14	1.97 (2)	C5–C4–Se1	116 (2)			C15–C14–Se11	116 (2)
Se12–C13	1.90 (2)	C4–C5–Se2	120 (2)			C14–C15–Se12	116 (2)
			β′-(BEDSe-TTF)$_2$IBr$_2$ (8)				
I–Br	2.704 (2)	C3–Se1–C7	99.3 (8)	S4–C6	1.72 (2)	C4–C3–Se1	127 (1)
Se1–C3	1.904 (15)	C4–Se2–C8	99.4 (7)	S4–C2	1.748 (14)	S1–C3–Se1	115.8 (8)
Se1–C7	1.93 (2)	C5–Se3–C9	94.2 (8)	C1–C2	1.34 (2)	C3–C4–S2	117 (1)
Se2–C4	1.898 (14)	C6–Se4–C10	101.4 (8)	C3–C4	1.37 (2)	C3–C4–Se2	130 (1)
Se2–C8	1.96 (2)	C3–S1–C1	95.7 (7)	C5–C6	1.34 (2)	S2–C4–Se2	113.3 (8)
Se3–C5	1.90 (2)	C1–S2–C4	96.0 (7)	C7–C8	1.38 (3)	C6–C5–S3	117 (1)
Se3–C9	1.95 (2)	C5–S3–C2	95.5 (7)	C9–C10	1.47 (3)	C6–C5–Se3	127 (1)
Se4–C6	1.91 (2)	C6–S4–C2	96.1 (8)			S3–C5–Se3	116.5 (9)
Se4–C10	1.96 (2)	C2–C1–S2	124 (1)			C5–C6–S4	118 (1)
S1–C3	1.72 (2)	C2–C1–S1	122 (1)			C5–C6–Se4	128 (1)
S1–C1	1.759 (14)	S2–C1–S1	114.5 (8)			S4–C6–Se4	114.6 (9)
S2–C1	1.724 (15)	C1–C2–S4	122 (1)			C8–C7–Se1	118 (2)
S2–C4	1.740 (14)	C1–C2–S3	124 (1)			C7–C8–Se2	119 (2)
S3–C5	1.752 (15)	S4–C2–S3	113.7 (9)			C10–C9–Se3	113 (1)
S3–C2	1.76 (2)	C4–C3–S1	117 (1)			C9–C10–Se4	117 (1)

[a] Primed atoms are related to unprimed ones by inversion through the middle of the central C–C bond.

BEDSe-TTF is used, with the appearance of an additional, intermediate structural type (AuI_2^- salt) which has not been observed with ET.

Electrical Conductivity and ESR Measurements. The room-temperature conductivity of β-(BEDSe-TTF)$_2$I$_3$ (**6**) is ~1 S/cm, which is comparable to that of the ET-based metals.[1] Variable-temperature conductivity measurements were carried out from 300 to 50 K, and the data recorded between 300 and 140 K are presented in Figure 7 on an expanded resistance scale. The resistivity curve displays three different regions. From 300 to 260 K, **6** exhibits metallic character. Between 260 and 140 K, it is semiconducting with a small activation energy of 0.028 eV (R_{140}/R_{300} = 2.0). Below 140 K, the resistivity increases rapidly, and at 50 K the resistance ratio (R_{50}/R_{300}) reaches 710.

The room-temperature ESR line shape of **6** is Lorentzian when the c^* axis (normal to the crystal plane) is parallel to the static magnetic field and Dysonian when the microwave electric field is parallel to the ab plane. The asymmetric Dysonian line shape is typical of a metal and

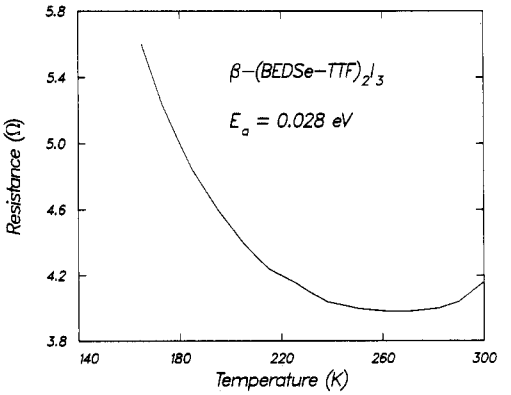

Figure 7. Resistance versus temperature plot for β-(BEDSe-TTF)$_2$I$_3$ (**6**).

Table V. Intermolecular Chalcogen• • •Chalcogen Contacts (angstroms) Less Than 3.8 Å

	β-(BEDSe-TTF)$_2$I$_3$ (6)		
Se1–Se3[a]	3.574 (1)	Se3–Se4[b]	3.724 (2)
Se1–Se2[b]	3.798 (2)	Se4–S2[d]	3.576 (2)
Se2–S1[c]	3.726 (2)	S1–S4[e]	3.652 (3)
Se2–Se4[d]	3.778 (2)	S1–S3[a]	3.713 (2)
Se3–S4[b]	3.438 (2)	S2–S3[e]	3.628 (3)
	(BEDSe-TTF)$_2$AuI$_2$ (7)		
Se1–S2[c]	3.767 (5)	Se2–Se12[f]	3.607 (3)
Se1–Se11[e]	3.542 (3)	S2–Se12[f]	3.724 (5)
Se1–S11[e]	3.698 (5)		
	β-(BEDSe-TTF)$_2$IBr$_2$ (8)		
Se1–Se2[b]	3.519 (3)	Se3–S4[b]	3.734 (5)
Se2–S1[c]	3.612 (4)	S2–S3[g]	3.668 (6)
Se3–Se4[b]	3.604 (3)		

[a] $1-x, 1-y, 1-z$. [b] $1+x, y, z$. [c] $-1+x, y, z$. [d] $-x, 2-y, 1-z$. [e] $-x, 1-y, 1-z$. [f] $1-x, -y, 1-z$. [g] $-x, -1-y, 1-z$.

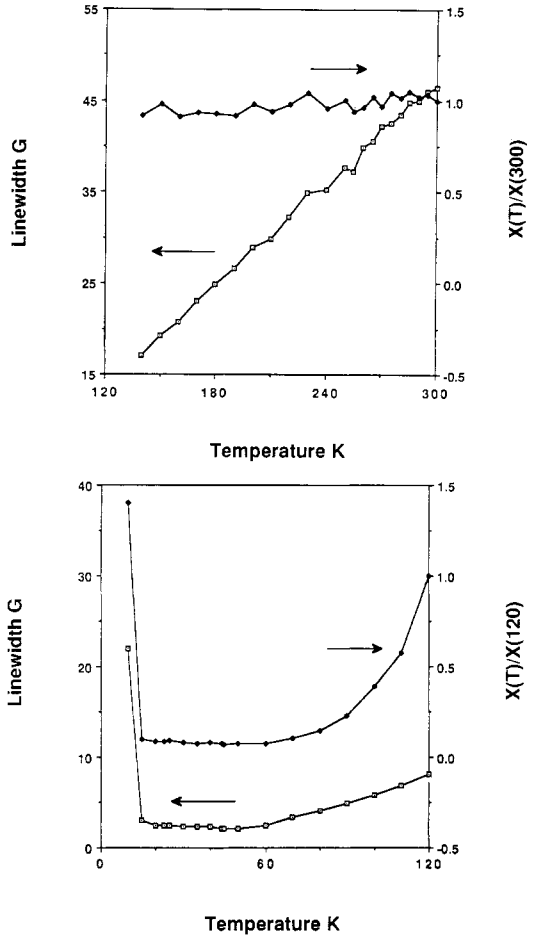

Figure 8. ESR peak-to-peak line width and relative spin susceptibility versus temperature for β-(BEDSe-TTF)$_2$I$_3$ (6): (top) 300–120 K; (bottom) 120–10 K.

has been observed in many ET-based synmetals.[37] The room-temperature Lorentzian line width of 6 is near 50 G. This is approximately 2.5 times larger than that of the sulfur-based β-(ET)$_2$X salts.[37] The broad line width, which is due partly to the presence of selenium atoms, suggests 2D character. Variable-temperature ESR measurements were performed on 6 (c^* perpendicular to the static magnetic field) from 300 to 10 K. As shown in Figure 8, top, the line width decreases monotonically with decreasing

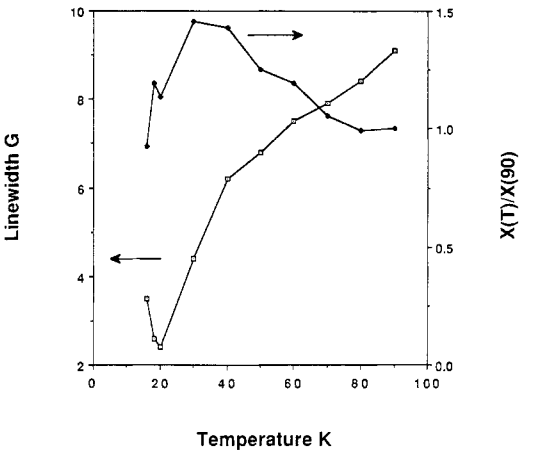

Figure 9. ESR line width and relative spin susceptibility versus temperature for (BEDSe-TTF)$_2$AuI$_2$ (7).

temperature between 300 and 140 K, and the spin susceptibility (χ) remains approximately constant. The conductivity measurements indicate that there is a very broad metal-to-semiconductor transition at about 260 K. The change in resistance from 300 to 140 K, however, is very small (a factor of ~2), so that the ESR measurements are apparently insensitive to this small change in conductivity and indicate metallic character over this temperature range. The systematic decrease in line width can be rationalized in terms of electron-scattering processes in the crystal lattice.[37] The ESR line width continues to decrease with decreasing temperature between 120 and 50 K and finally becomes constant (Figure 8, bottom). The spin susceptibility in the same temperature range drops 1 order of magnitude, which is indicative of an insulating ground state. The ESR spectra below 10 K appear to be dominated by paramagnetic impurities. In summary, both the ESR and the conductivity measurements on β-(BEDSe-TTF)$_2$I$_3$ indicate a metallic state near room temperature and an insulating ground state at low temperatures, although the transition temperature is not consistently defined by these two different measurements.

The physical properties of 7 and 8 are similar to those of β′-(ET)$_2$X, X$^-$ = ICl_2^- and $AuCl_2^-$.[35,36] The room-temperature conductivity of (BEDSe-TTF)$_2$AuI$_2$ (7) is $\sigma_{300} \sim 6.2 \times 10^{-2}$ S/cm. It is a semiconductor with an E_a of 0.13 eV. The room-temperature ESR line width of 7 is narrow (16–19 G), which indicates low dimensionality. The ESR signal of 7 was monitored from 100 to 14 K with the c^* axis parallel to the static magnetic field. As shown in Figure 9, the peak-to-peak line width decreases from 9.1 G at 90 K to a minimum of 2.4 G at 20 K. Below 20 K, the line width broadens and the spin susceptibility drops rapidly. The ESR absorption disappears completely near 14 K. Apparently, antiferromagnetic coupling starts to dominate below ~20 K. β′-(BEDSe-TTF)$_2$IBr$_2$ (8) is a semiconductor with $\sigma_{300} \sim 3 \times 10^{-3}$ S/cm and E_a of 0.09 eV. The room-temperature ESR line shape of 8 is Lorentzian, and the line width is 23–29 G, which is about 50% smaller than in the corresponding I_3^- salt. The narrower line width suggests lower dimensionality. The variable-temperature ESR properties have been measured from 300 to 10 K with c^* axis parallel to the static magnetic field. As shown in Figure 10, the peak-to-peak line width decreases monotonically from 24.8 G at 300 K to a minimum of 2.1 G at 12 K. The spin susceptibility increases slightly with decreasing temperature, reaches a broad maximum (120% of its 300 K value) at 100 K, and then decreases slightly from 100 to 12 K (70% of the 300 K value). Below 12 K, the line width increases again and the spin susceptibility

(37) Venturini, E. L.; Azevedo, J. E.; Schirber, J. E.; Williams, J. M.; Wang, H. H. *Phys. Rev. B. Condens. Matter* **1985**, *32*, 2819.

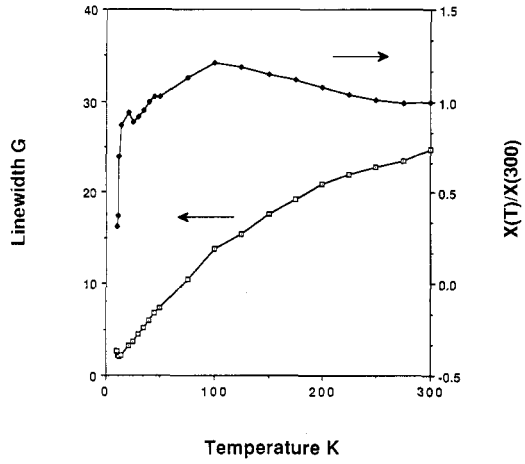

Figure 10. ESR peak-to-peak line width and relative spin susceptibility versus temperature for β'-(BEDSe-TTF)$_2$IBr$_2$ (8).

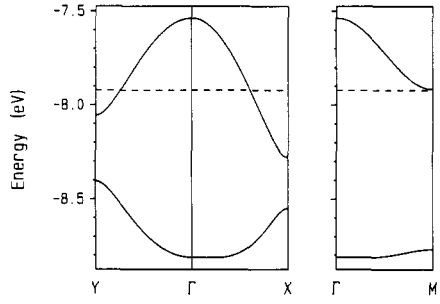

Figure 11. Dispersion relations of the two highest occupied bands of β-(BEDSe-TTF)$_2$I$_3$, where the dashed line refers to the Fermi level. Γ = (0,0), $X = (a^*/2,0)$, $Y = (0,b^*/2)$, and $M = (-a^*/2,b^*/2)$.

drops rapidly to 30% of the 300 K value at 10 K. A slight increase in g value is also noted around 12 K. This behavior is consistent with an antiferromagnetically coupled transition near 12 K. From the broad maximum in the susceptibility near 100 K, an exchange constant ($J/k \sim$ 80 K), which is based on a pair Hamiltonian of the form $-2J\mathbf{S}_i\cdot\mathbf{S}_{i+1}$, can be estimated.[38]

FT-IR Reflectance Measurements. The infrared reflectance spectrum of **6** was measured in the 4000–600-cm^{-1} region by use of microscopic techniques, employing a single crystal. The spectrum shows a broad band that increases in reflectance with decreasing frequency and has vibrational features between 1200 and 1400 cm^{-1}. When the spectrum is plotted in absorbance units, an absorption dip occurs near 1268 cm^{-1}. Similar absorption dips have been observed in β-(ET)$_2$X (1280 cm^{-1}, X$^-$ = I_3^-, AuI_2^-, IBr_2^-) salts at room temperature but not in α-(ET)$_2$X (X$^-$ = I_3^-, IBr_2^-) salts and have been utilized to identify the α- and β-phases.[39] The absorption dip in the ET-based materials has been attributed to an IR-active C–C–H bending mode. The frequency of this dip appears to be sensitive to the strength of the C–C–H···X interactions and to the electronegativity of the anion.[39] The frequency of the absorption dip in **6** compares closely to that of (PT)$_2$I$_3$ (1270 cm^{-1}) but not β-(ET)$_2$I$_3$. This may be due to the conformational preferences b and c (Figure 2) of the terminal ethylene groups. The infrared spectrum of **7** in the 4000–600-cm^{-1} region does not reveal a broad-band reflectance spectrum. The corresponding absorption dip in **8** (1272 cm^{-1}) is a few wavenumbers higher than that of **6**. This trend in proceeding from the β- to β'-structural type has also been observed in the β-(ET)$_2$X complexes.

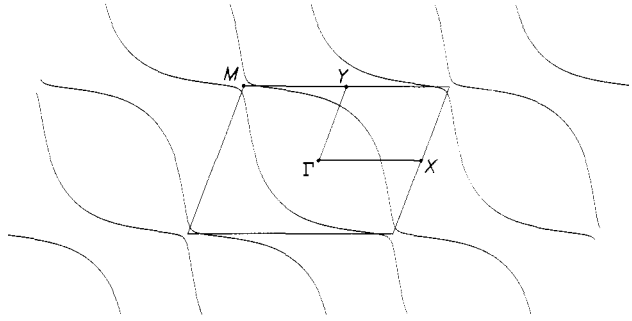

Figure 12. Fermi surface associated with the half-filled band of Figure 11.

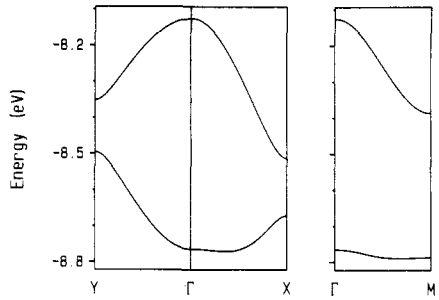

Figure 13. Dispersion relations of the two highest occupied bands of (BEDSe-TTF)$_2$AuI$_2$ (**7**), where the upper band is half-filled.

Band Electronic Structures. In an attempt to understand the electrical properties of the (BEDSe-TTF)$_2$X salts discussed above, tight-binding band calculations[18] were performed on the donor layers. The calculations were based upon the extended Hückel method[40] as described elsewhere[18] and utilized double-ζ Slater type orbitals for the s and p orbitals of C, S, and Se atoms.[41]

Figure 11 shows the dispersion relations of the two highest occupied bands of β-(BEDSe-TTF)$_2$I$_3$, which are mainly derived from the HOMO of each donor molecule. With the oxidation scheme of (BEDSe-TTF)$_2^+$, the upper band is half-filled. Since the I_3^- salt is metallic above 260 K, this band is half-filled. The Fermi surface associated with this band is shown in Figure 12, where the parallelogram represents a primitive unit cell in reciprocal space. The Fermi surface is almost closed near M, so that β-(BEDSe-TTF)$_2$I$_3$ is expected to be a nearly 2D metal. The calculated Fermi surface does not have a good nesting. The observed metal–insulator transition of the I_3^- salt near 260 K must be associated with the destruction of the above Fermi surface, which can be brought about by a lattice dimerization.

As shown in Figure 13, the dispersion relations for the two highest occupied bands of (BEDSe-TTF)$_2$AuI$_2$ **7** are similar to those of β-(BEDSe-TTF)$_2$I$_3$. However, the band widths of the former are narrower. In addition, the upper and the lower bands of **7** have contributions largely from

(38) De Jongh, L. J. In *Magneto-Structural Correlations in Exchange Coupled Systems*; Willett, R. D., Galleschi, D., Kahn, O., Eds.; NATO ASI Series C140, 1985; p 1.

(39) Ferraro, J. R.; Wang, H. H.; Ryan, J.; Williams, J. M. *Appl. Spectrosc.* **1987**, *41*, 1377.

(40) Hoffmann, R. *J. Chem. Phys.* **1963**, *39*, 1397.

(41) For each S, C, and Se, each atomic orbital μ was represented by a linear combination of two Slater-type orbitals of exponents ζ_μ and ζ'_μ with weighting coefficients c_μ, and c'_μ, respectively.[42] The ζ_μ, ζ'_μ, c_μ, c'_μ, and $H_{\mu\mu}$ (valence-shell ionization potentials) values employed were, respectively, 3.139, 1.900, 0.5822, 0.4846, and −20.5 eV for Se 4s and 2.715, 1.511, 0.5347, 0.5553, and −14.4 eV for Se 4p. The atomic parameters for S, C, and H were taken from ref 18. The off-diagonal $H_{\mu\nu}$ values were calculated from a modified Wolfsberg-Helmholz formula.[43]

(42) Clementi, E.; Roetti, C. *At. Data Nucl. Data Tables* **1974**, *14*, 177.

(43) Ammeter, J. H.; Bürgi, H.-B.; Thibeault, J. C.; Hoffmann, R. J. *Am. Chem. Soc.* **1978**, *100*, 3686.

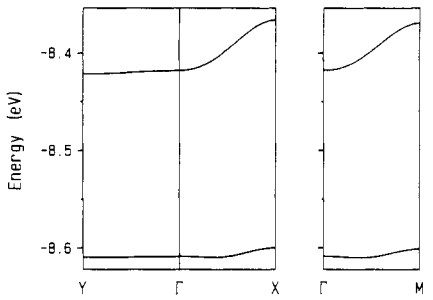

Figure 14. Dispersion relations of the two highest occupied bands of β'-(BEDSe-TTF)$_2$IBr$_2$ (8), where the upper band is half-filled.

the HOMOs of molecules B and A, respectively. This is reasonable, because the HOMO of molecule B is calculated to be higher lying in energy than that of molecule A (by about 0.2 eV). The semiconducting properties of **7** can be explained by an extreme oxidation formalism A^0B^+, i.e., the half-filled upper band of Figure 13 is not metallic but is magnetic insulating.[44] Unfortunately, the bond-length error limits of the crystal structure of **7** are too large to detect any differences in the two crystallographically independent donor molecules to test this hypothesis. Differences in the oxidation states may be favored by the different electrostatic potential due to anion lattice at the donor sites of A and B. Figure 14 shows the dispersion relations for the two highest occupied bands of β'-(BEDSe-TTF)$_2$IBr$_2$. The band widths are extremely narrow, so that the half-filled upper band is magnetic insulating. Simply speaking, the donor layer is made up of dimerized radical-cation units (BEDSe-TTF)$_2^+$.

Conclusions

Three BEDSe-TTF-based salts with linear anions (I_3^-, AuI_2^-, and IBr_2^-) have been prepared by electrocrystallization and characterized by X-ray crystallography, electrical conductivity measurements, variable-temperature ESR studies, and FT-IR reflectance measurements. The desirable 2:1 stoichiometry, which often results in superconductivity in β-(ET)$_2$X salts, was obtained in all three cases. The β-packing motif, which is also found in many of the ET-based organic superconductors, was observed only in the case of β-(BEDSe-TTF)$_2$I$_3$. The IBr_2^- salt packs in the β'-mode, and the AuI_2^- compound adopts a β-like motif that has not been observed previously. β-(BEDSe-TTF)$_2$I$_3$ is metallic at room temperature but undergoes a metal–semiconductor transition at about 260 K. ESR studies at very low temperatures suggest that the triiodide has an insulator ground state. This behavior contrasts sharply with that of β-(ET)$_2$I$_3$, which is metallic down to 1.5 K, where it becomes superconducting. The pronounced difference between the two β-salts is very likely related to the increase in key interstack chalcogen nonbonded distances (Table V) in β-(BEDSe-TTF)$_2$I$_3$ vs β-(ET)$_2$I$_3$ that are brought about by the slightly larger size of the four outer seleniums and, perhaps, the conformational preferences of the terminal ethylene groups (conformations b and c in Figure 2). (BEDSe-TTF)$_2$AuI$_2$ and β'-(BEDSe-TTF)$_2$IBr$_2$ are semiconductors at room temperature, and both undergo antiferromagnetic coupling to insulator ground states at low temperatures. Tight-binding band calculations, which were performed on the donor layers of the (BEDSe-TTF)$_2$X salts, reveal a nearly 2D Fermi surface for the I_3^- salt, a possible charge localization in the AuI_2^- salt, and a magnetic insulating band structure for the IBr_2^- salt. Generally speaking, BEDSe-TTF and ET are sufficiently different that the replacement of the donors leads to salts with different structures and different physical properties. However, we believe that it is possible to find new organic metals and superconductors with donor molecules that are slight variants of the successful ET donor.

Acknowledgment. Work at Argonne National Laboratory is sponsored by the U.S. Department of Energy (DOE), Office of Basic Energy Sciences, Division of Materials Sciences, under Contracts W-31-109-ENG-38. L. K.M. is a Scientist in Residence, sponsored by the Argonne Division of Educational Programs, on leave from the Department of Chemistry, Indiana University, Bloomington, IN. C.S.C., R.L.R., and J.R.W. are student research participants sponsored by the Argonne Division of Educational Programs from Humboldt State University, Arcata, CA, Carnegie-Mellon University, Pittsburgh, PA, and Transylvania University, Lexington, KY, respectively. Research at North Carolina State University is in part supported by DOE, Office of Basic Energy Sciences, Division of Material Sciences, under Grant DE-FG05-86ER45259. We express our appreciation for computing time on the ER-Cray X-MP computer, made available by DOE. Thanks and appreciation are extended to Digilab Division of Bio-Rad, Cambridge, MA, for the use of their equipment for the reflectance measurements and to Steve Hill of Digilab for assistance in making these measurements.

Supplementary Material Available: Tables of crystal structure data collection and refinement parameters, atomic coordinates and anisotropic thermal parameters for β-(BEDSe-TTF)$_2$I$_3$, (BEDSe-TTF)$_2$AuI$_2$, and β'-(BEDSe-TTF)$_2$IBr$_2$, and a countour difference map for (BEDSe-TTF)$_2$AuI$_2$ (5 pages); observed and calculated structure factors for the above compounds (17 pages). Ordering information is given on any current masthead page.

(44) (a) Whangbo, M.-H. In *Crystal Chemistry and Properties of Low-Dimensional Solids*; Rouxel, J., Ed.; Reidel: Dordrecht, Netherlands, 1986; p 27. (b) Whangbo, M.-H. *Acc. Chem. Res.* **1983**, *16*, 95.